Target design for energetic ion assisted fast ignition

H. Sakagami[1], T. Johzaki[2], A. Sunahara[3], H. Nagatomo[4]

[1]*Fundamental Physics Simulation Div., National Institute for Fusion Science, Toki, Japan*

[2]*Mechanical Systems Engineering, Hiroshima University, Higashihiroshima, Japan*

[3]*Institute for Laser Technology, Osaka, Japan*

[4]*Institute of Laser Engineering, Osaka University, Osaka, Japan*

1. Introduction

A fuel target is imploded by long-pulse implosion lasers and its compressed core is heated by a short-pulse ultrahigh-intense laser in the fast ignition scheme. FIREX experiments have started at ILE, Osaka University to demonstrate this scheme using Au cone-guided targets. Efficient core heating mechanisms have not been, however, clarified yet, and we have been promoting the Fast Ignition Integrated Interconnecting code (FI^3) project to boldly explore fast ignition frontiers. 2D PIC simulations and basic experiments indicate that the coupling efficiency from fast electrons to the core is quite low even that from the heating laser to fast electrons is generally high because the divergence angle of fast electrons is large and their slope temperature is too high to deposit the energy into the core [1]. Thus a relatively small enhancement in neutron yield was achieved in experiments.

To mitigate this critical issue, a plastic (CH) thin film or low-density foam, which can generate energetic not only proton (H^+) but also carbon (C^{6+}) beams, is introduced into the cone-guided target as a controllable ion beam generator, expecting additional core heating by ions. There are two well-known ion acceleration mechanisms. With the thin film generator, ions are accelerated by the sheath field at the rear surface [2]. On the other hand, ions are also accelerated by the Ponderomotive force at the front surface [3] of a low-density foam target. In both cases, the CH generators are placed close to the cone tip in order to shorten the distance between the ion generation point and the compressed core. This simple design can reduce core-arrival time lags due to different ion energies, and we can accept ion beams with wide energy range. Time lags between fast electrons and energetic ions can also be reduced, and this design makes it easy to introduce the ion beam generator into FIREX experiments combining with currently used cone-guided targets. Electron and ion beam characteristics are investigated by 2D PIC simulations and core heating properties are evaluated by integrated simulations by 1D RFP-Hydro code [4].

2. Sheath Field Acceleration

As the heating laser, LFEX, in FIREX project is designed to have 10 ps pulse length and the cone tip is placed 50 μm away from the implosion center, we assume that ion beams should propagate 60 μm long within 5 ps time lag. So ions with the speed faster than 0.04 of the light speed, namely H^+ with the energy higher than 0.7 MeV or C^{6+} higher than 9 MeV, can be used to additionally heat the core.

To adapt the sheath field acceleration, we introduce the thin film ion generator inside the cone as shown in Fig. 1 (a). The Au cone plasma (Z=30, A=197, $20n_{cr}$, 60 degree open angle, 10 μm tip width) is introduced and the CH thin film (Z=6, A=12, $17.14n_{cr}$ and Z=1, A=1, $2.86n_{cr}$, 4.5 μm thickness) is placed 5 μm away from the cone tip surface. When the sheath field is induced, dense background electrons in the Au plasma are pulled and injected into the CH thin film and it results in reducing the sheath field. Therefore 0.5 μm gaps between the Au and the CH thin film are introduced to prevent the electron flow as shown in Fig. 1 (b). Ion acceleration by the sheath field is incompatible with electron acceleration, so maintained sheath field by the gap prevents fast electrons from propagating forward, and it leads to reduction of core heating by fast electrons. If the ion generator is destroyed after acceleration, the heating laser can interact with the cone tip to generate more fast electrons. Lower density CH thin film leads to earlier destruction, but it cannot maintain the sheath field. Thus we introduce slits as shown in Fig. 1 (c), which are narrow enough that the laser cannot propagate, so that the CH thin film can be destroyed earlier.

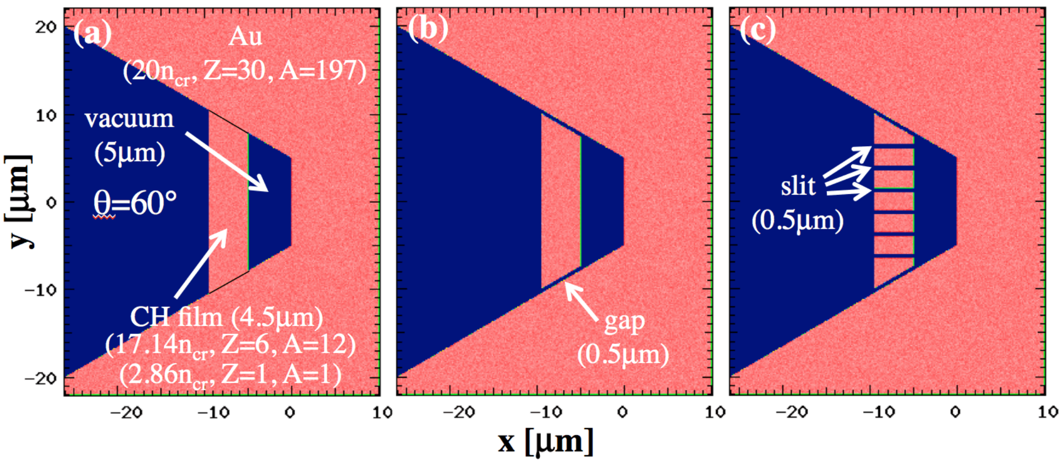

Fig. 1 Targets for energetic ion beam assisted fast ignition with sheath field acceleration (a) without gap, (b) with gap and (c) slit with gap.

The heating laser is set to λ_L=1.06 μm, I_L=10^{20} W/cm^2, τ_{rise}=τ_{fall}=50 fs, τ_{flat}=400 fs and ϕ_{FWHM}=10 μm super-Gaussian with α=5. Fast electrons and energetic ions are observed at 1 μm behind of the cone tip surface with 30 (±15) μm width. To ignore a circulation of fast electrons, we introduce an artificial cooling region (1 μm width), in which fast electrons are gradually cooled down to the initial temperature, behind the observation region, top and bottom regions of the Au plasma. Using the time-dependent profiles of fast electrons and ions, which are observed in 0 < y < 3 μm in 2D PIC code, into 1D RFP-Hydro code, we carried out integrated simulations to evaluate the core heating properties, including 7 μm transport in the Au cone tip. Time evolutions of averaged core electron temperatures are shown in Fig. 2 (a) for all 3 cases. As electrons finish to heat the core but ions do not reach the core yet due to slow speed, electrons play a dominant role in core heating before the inflection point. After that, ions finally reach and dominantly heat the core instead of electrons. Enhancements of averaged core electron temperatures are summarized in Table 1. In the case with the gap, enhancement by ions is larger than that without the gap. On the other hand, the forward propagation of fast electrons is disturbed by the same sheath field, and electron heating is reduced. In the slit with gap case, the ion generator is successfully destroyed after ion acceleration and the heating laser can interact with the cone tip. So fast electrons are enhanced after the destruction, and the number of fast electrons that are suitable to heat the core is recovered.

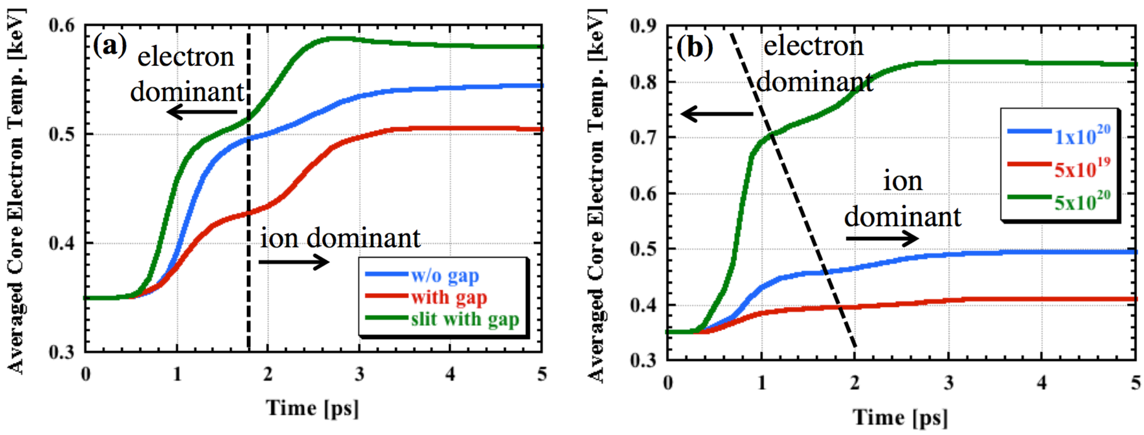

Fig.2 Time evolutions of averaged core electron temperatures for (a) sheath field acceleration and (b) Ponderomotive force acceleration.

Table 1. Summary of enhancement of averaged core electron temperature for sheath field acceleration.

		w/o gap	with gap	slit with gap
Temperature increment keV	e only	0.15	0.08	0.16
	$e + H^{+} + C^{6+}$	0.19	0.16	0.23
Enhancement by ions %		27	100	44

3. Ponderomotive force acceleration

For the Ponderomotive force acceleration, we introduce the low-density foam ion generator in front of the cone tip surface as shown in Fig. 3. As the scaling of ion velocity by the Ponderomotive force is given in $v_i \propto (I_L/n_e)^{1/2} (Z/A)^{1/2}$ [3], lower density gives higher energy, but it should be larger than relativistic critical density and $n_e \sim \gamma\, n_{cr} \propto (I_L)^{1/2}$ where γ is the Lorentz factor of quivering electrons under the laser field and n_{cr} is the critical density. Thus we chose the electron density of the foam to $\gamma\, n_{cr}$ (6.12, 8.60 and 19.13n_{cr} for I_L=5x10^{19}, 1x10^{20} and 5x10^{20} W/cm^2, respectively), and maximum ion energy scaling is written as $E_i \propto (I_L)^{1/2} Z$. Another simulation parameters are same as previous case. Time evolutions of averaged core electron temperatures are shown in Fig. 2 (b) and enhancements of averaged core electron temperatures are summarized in Table 2 for different laser intensity. Estimated scaling of maximum ion energy on the laser intensity roughly agrees with simulation result, but the core electron temperature increment is not proportional to the laser energy or laser intensity.

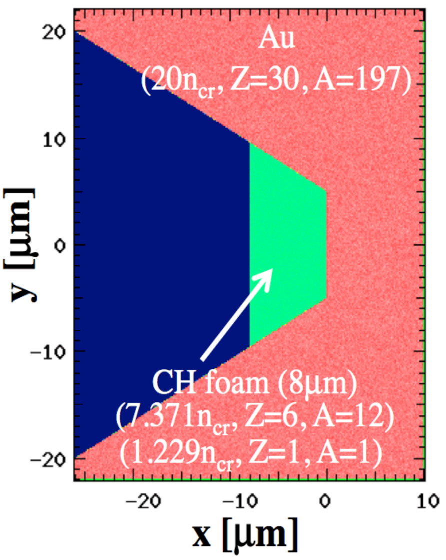

Fig. 3 Targets for energetic ion beam assisted fast ignition with Ponderomotive force acceleration for I_L=1x10^{20} W/cm^2.

Table 2. Summary of enhancement of averaged core electron temperature for Ponderomotive acceleration.

Laser Intensity W/cm^2		5x10^{19}	1x10^{20}	5x10^{20}
Temperature increment keV	e only	0.05	0.11	0.35
	e + H^+ + C^{6+}	0.06	0.15	0.48
Enhancement by ions %		20	36	37

Acknowledgments

This work was partially supported by JSPS Grant-in-Aid for Scientific Research (C)(25400539).

References

[1] T. Johzaki, et al., Nucl. Fusion **51**, 073022 (2011).

[2] R. A. Snavely, et al., Phys. Rev. Lett. **85**, 2945 (2000).

[3] S. C. Wilks, et al., Phys. Rev. Lett. **69**, 1383 (1992).

[4] H. Sakagami, et al., Nucl. Fusion **49**, 075026 (2009).